NORMAL FREQUENCIES OF A STRING VIBRATING AT LARGE AMPLITUDES

by

David C. Ripplinger

A senior thesis submitted to the faculty of

Brigham Young University

in partial fulfillment of the requirements for the degree of

Bachelor of Science

Department of Physics and Astronomy

Brigham Young University

August 2009

BRIGHAM YOUNG UNIVERSITY

DEPARTMENT APPROVAL

of a senior thesis submitted by

David C. Ripplinger

This thesis has been reviewed by the research advisor, research coordinator, and department chair and has been found to be satisfactory.

Aug. 10, 2009	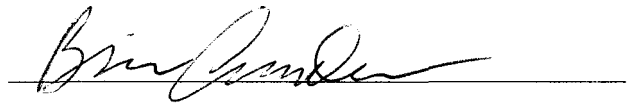
Date	Brian E. Anderson, Advisor
Date	Eric Hintz, Research Coordinator
Date	Ross L. Spencer, Chair

ABSTRACT

NORMAL FREQUENCIES OF A STRING VIBRATING AT LARGE AMPLITUDES

David C. Ripplinger

Department of Physics and Astronomy

Bachelor of Science

Large displacement amplitudes in a freely vibrating string require that one consider the dynamic tension of the string to determine the normal frequencies instead of the commonly used equilibrium tension approximation. Large amplitudes can cause these frequencies to be significantly sharper. A theoretical model is presented to provide a more accurate approximation of the tension, which includes a correction term that is proportional to the total energy in the string. Experiments have been performed using a repeatable plucking mechanism on a monochord string apparatus. The motion of the plucked string was recorded for both vertical and horizontal displacements using a high speed camera. The instantaneous total energy in the string was then calculated as the string's motion decayed, using the instantaneous frequency method and a narrow band-pass Bessel filter. A comparison is made between the model and the experimental results of the total energy in the string as a function of time. The data show that when a string is plucked at large displacement amplitudes the partial frequencies can be as much as 83 cents sharp relative to their stable frequency values.

ACKNOWLEDGMENTS

This research was made possible by funding from the BYU Department of Physics and Astronomy, by the invaluable aid of my advisors, Dr. Tim Leishman and Dr. Brian Anderson, and by the generosity of Dr. Scott Thomson and the BYU Mechanical Engineering Department in lending their high speed camera. A special thanks is due to Dr. William Strong for his expertise in musical acoustics that he made freely available, and to Brian Thornock, a fellow student in the BYU Acoustics Research Group, who was key in getting the instantaneous frequency method to work using the Bessel filter. Finally, I thank my wife for her love and support during this period of strenuous research.

Contents

List of Figures

I. Introduction

In the field of musical acoustics, the study of string vibrations is a major area of interest, since many musical instruments employ strings. The low-amplitude displacement solution to a freely vibrating string fixed at both ends is well known and straightforward (see Section II). However, when the string's displacement amplitudes become larger, the commonly used low-amplitude approximation is insufficient to accurately describe the normal modes of the string and their corresponding partial frequencies.

Fletcher developed a theoretical expression to predict the partial frequencies of a piano string by including a fourth-order stiffness term in the differential equations of motion,[1] but this correction was for low-amplitude displacement and is unrelated to the large-amplitude problem. Anderson and Strong determined the effect of Fletcher's inharmonicity on the pitch of piano tones,[2] but their work did not address large-amplitude displacements either. Other previous research has focused on studying nonlinear effects in the motion of a string. Morse and Ingard derived coupled differential equations that govern the motion of a string in three dimensions at large amplitudes.[3] Anand then solved these equations (with damping) for the specific case of sinusoidal motion and demonstrated that any point on the string traces a slowly decaying elliptical path at a frequency proportional to a given nonlinearity parameter.[4] Bilbao, on the other hand, developed a numerical method to solve the equations that uses conservation of energy to achieve global stability for the algorithm.[5] He also mentioned that the most noticeable nonlinear effect was an increase in gross propagation speed (directly related to the observed partial frequencies); however, he did not quantify this in terms of known values, such as energy. To date, nothing known to the author has been published that describes how the pitch, or the normal frequencies (or partials) of a string may be affected by larger amplitudes.

This work presents a theoretical model, adapted from Morse and Ingard, which describes the partial frequency correction due to large amplitudes. It then presents an experiment to test the accuracy of the theory. The model is based on the idea that when the dynamic tension is approximated as a constant, it is more accurate to take the time and spatial averages instead of the more widely used equilibrium tension, which is its minimum value over all space and time. This new approximation yields a correction term to the partial frequencies that is proportional to the total energy in the string. It will be shown in Section V that even moderate initial amplitudes in a vibrating string, commonly seen in musical performance, indeed lead to a deviation of several cents (hundredths of a semitone) from the low-amplitude partial frequencies.

In conducting the experiment, the instantaneous frequency (IF) method is employed in order to track transient partial frequencies of the plucked string, since standard fast Fourier transform techniques yield insufficient frequency resolution over one period of the fundamental frequency. One of the first publications that introduced the concept of IF was authored by Carson and Fry in 1937.[6] Several modifications were made in subsequent publications, leading to the various definitions of IF today. The definition used in this work was introduced by Ville.[7] Boashash provided a comprehensive study on the nature of the IF method, its historical development and its applications.[8,9] Suzuki et. al. demonstrated the use of the IF method on frequency-modulated and amplitude-modulated sinusoids, from an analytical perspective.[10] They also calculated the error introduced by the IF method at the onset of a finite sinusoidal signal, where the known frequency is over estimated by a factor of two. The IF method was further employed by Rossi and Girolami to study musical phenomena of piano tones, such as beats caused by two closely spaced partials.[11] They used a narrow-band Gaussian filter over the partial frequency of interest, offering little explanation for this choice. There is no standard method of filtering a signal before using the IF method; however, the experiments conducted in this work demonstrated that a Bessel filter used before computing the IF produced the most reliable results, accurately estimating known frequencies over almost the entire range of a signal,

including the critically important beginning portion (the attack).

The prediction and high-resolution measurement of frequency drift is extremely useful in better understanding the musical aspect of stringed instruments when plucked or struck hard, as well as in improving the science of tuning musical instruments.

II. Theoretical model

Consider a freely vibrating string of length l, fixed at both ends. The forces that act on the string can be determined by analyzing Fig. 1, which shows a very small portion of the string with the opposing tensions acting on it. The net force may be expressed in terms of the Cartesian components x and y,

$$F_y = T\sin(\theta + d\theta) - T\sin\theta \approx T\,d\theta, \tag{1}$$

$$F_x = T\cos(\theta + d\theta) - T\cos\theta \approx 0, \tag{2}$$

where T is the tension, θ is the angle between the tension vector and the horizontal axis on the left side of the string, and $\theta + d\theta$ is the angle between the tension vector and the horizontal axis on the right side of the string. The tension is a function of x and time t, but for relatively low amplitudes, the oscillations in this function are small enough that it may be approximated as a constant value. It is well known that Eq. (1) leads to the linear wave equation,

$$\frac{\partial^2 y}{\partial t^2} = c^2 \frac{\partial^2 y}{\partial x^2}, \tag{3}$$

where y is the vertical displacement of the string, $c = \sqrt{T/\mu}$ is the transverse wave speed and μ is the linear mass density of the string.[12] The general solution to Eq. (3), along with the boundary conditions $y(0,t) = y(l,t) = 0$, may be expressed as

$$y(x,t) = \sum_{n=1}^{\infty} a_n \sin\left(\frac{n\pi x}{l}\right)\cos\left(\frac{n\pi c t}{l} - \phi_n\right), \tag{4}$$

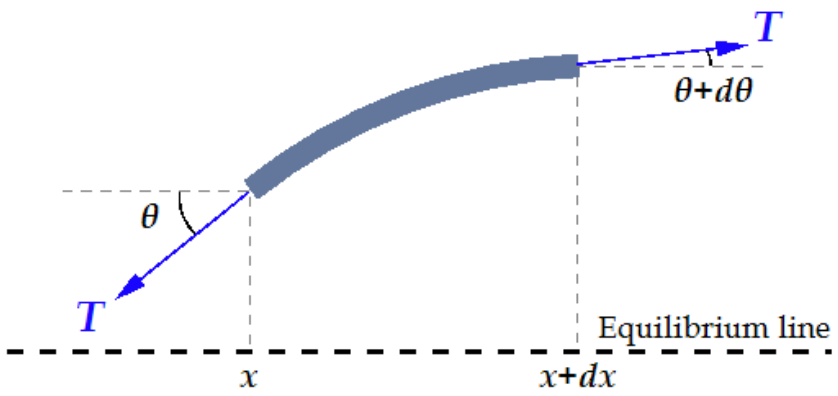

FIG. 1. Forces acting on a small section of a freely vibrating string.

where n is the index number of each normal mode and a_n and ϕ_n represent the amplitude and phase, respectively. The latter are determined by initial conditions. The partial frequencies corresponding to the normal modes are then

$$\nu_n = \frac{nc}{2l} = \frac{n}{2l}\sqrt{\frac{T}{\mu}}. \tag{5}$$

Morse and Ingard[3] claim that the dynamic tension is given by

$$T(x,t) = T_0 + QA\left(\left|\frac{\partial \mathbf{R}}{\partial x}\right| - 1\right), \tag{6}$$

where T_0 is the equilibrium tension when the string is not in motion, Q is the Young's modulus for the string material, A is the cross-sectional area of the string, and $\mathbf{R}$ is the position vector from the origin to the point on the string which was at $(x, 0, 0)$ in equilibrium. This formula is generalized to three dimensions. It can be verified by geometrical arguments and application of Hooke's law for an ideal spring (see Appendix A). The conventional solution to Eq. (3) approximates Eq. (6) by its zero*th* order term T_0. However, the dynamic tension consists of small oscillations in x and t with a minimum value of T_0. It is more precise to approximate Eq. (6) by its time and spatial averages. To calculate

the averages, we first approximate $\left|\partial\mathbf{R}/\partial x\right|$ to first order, assuming that longitudinal displacement is much less than transverse displacement. Let $\mathbf{R} = x\mathbf{e}_x + \mathbf{r}(x,t)$, where $\mathbf{r}$ is the displacement vector from equilibrium, denoted as $\mathbf{r}(x,t) = \xi(x,t)\mathbf{e}_x + \eta(x,t)\mathbf{e}_y + \zeta(x,t)\mathbf{e}_z$. Then

$$\begin{aligned}\left|\frac{\partial\mathbf{R}}{\partial x}\right| &= \sqrt{\left(1+\frac{\partial\xi}{\partial x}\right)^2 + \left(\frac{\partial\eta}{\partial x}\right)^2 + \left(\frac{\partial\zeta}{\partial x}\right)^2} \\ &\approx 1 + \frac{1}{2}\left(\frac{\partial\eta}{\partial x}\right)^2 + \frac{1}{2}\left(\frac{\partial\zeta}{\partial x}\right)^2,\end{aligned} \tag{7}$$

so that

$$T(x,t) = T_0 + \frac{1}{2}QA\left(\left(\frac{\partial\eta}{\partial x}\right)^2 + \left(\frac{\partial\zeta}{\partial x}\right)^2\right), \tag{8}$$

and the averages are

$$\left\langle\left\langle T\right\rangle_t\right\rangle_x = T_0 + \frac{1}{2}QA\left(\left\langle\left\langle\left(\frac{\partial\eta}{\partial x}\right)^2\right\rangle_t\right\rangle_x + \left\langle\left\langle\left(\frac{\partial\zeta}{\partial x}\right)^2\right\rangle_t\right\rangle_x\right), \tag{9}$$

where the double angular brackets indicate both time and spatial averages. It turns out that

$$\begin{aligned}\left\langle\left\langle\left(\frac{\partial\eta}{\partial x}\right)^2\right\rangle_t\right\rangle_x + \left\langle\left\langle\left(\frac{\partial\zeta}{\partial x}\right)^2\right\rangle_t\right\rangle_x &= \frac{E_y + E_z}{Tl} \\ &= \frac{E}{Tl} \approx \frac{E}{T_0 l},\end{aligned} \tag{10}$$

where E_y and E_z are the energies for the respective dimensions of motion and E is the total energy in the string (see Appendix B), so that

$$\langle\langle T \rangle\rangle = T_0 \left[1 + \frac{1}{2} \left(\frac{QA}{T_0} \right) \left(\frac{E}{T_0 l} \right) \right]. \tag{11}$$

Using Eq. (11) in Eq. (5), we find that large amplitudes cause the partial frequencies ν_n to deviate from their stable values $\nu_n^{(0)}$ by the ratio

$$\frac{\nu_n}{\nu_n^{(0)}} = \sqrt{1+\varepsilon}\ , \tag{12}$$

where the correction parameter $\varepsilon = \frac{1}{2}(QA/T_0)(E/T_0 l)$ is proportional to the total energy in the string.

In musical acoustics, frequency deviations are often expressed in cents C (100 cents is equal to a semitone interval in an equally tempered 12-tone scale). The shifted frequencies differ from the stable values, in cents, according to

$$\begin{aligned} C &= 1200 \log_2 \left(\frac{\nu_n}{\nu_n^{(0)}} \right) \\ &= 1200 \log_2 \sqrt{1+\varepsilon} \\ &= 600 \log_2 (1+\varepsilon)\ . \end{aligned} \tag{13}$$

To get an idea of how significant a change can happen in practice due to ε, let us take a look at what it would take to produce a deviation of an entire semitone from the stable partial frequencies:

$$\begin{aligned} &C = 100 = 600 \log_2 (1+\varepsilon)\ , \\ &\varepsilon = 2^{1/6} - 1 \approx 0.12246\ . \end{aligned} \tag{14}$$

For piano strings, $QA/T_0 = 500$ is a typical value and the factor $E/T_0 l = 2.4492 \times 10^{-4}$ is still rather small. If only the first partial is present, its amplitude would equal $a_1 = 0.01 l$ (this is calculated using Eq. (B.4), in Appendix B). Thus, a significant, sometimes dra-

matic, effect in many applied cases can be expected, such as is the case for several musical instruments.

III. Instantaneous frequency method

If it were possible to have a freely vibrating string continue with the same amplitudes indefinitely, we could simply observe the acoustic signal or the vibration of the string over a long period of time and obtain very high accuracy in the frequency domain, using a fast Fourier transform (FFT), for some known constant energy. But every real freely vibrating string is subject to damping forces, so the amplitudes must decrease over time. Therefore, in order to experimentally measure how the partials of a freely vibrating string depend on its total energy, it is necessary to track these partials with high resolution in both the time and frequency domains as the string decays. It is fundamentally impossible to obtain perfect resolution with 100% reliability in both domains simultaneously, due to the time-frequency uncertainty principle. However, several methods in signal processing may be used to minimize this uncertainty for specific kinds of signals, or in order to extract a specific piece of information.

Conventionally, if one needed to measure the frequencies incorporated in a given signal, one would utilize the standard Fourier transform to convert the time data into the frequency domain. However, the Fourier transform itself has many limitations, especially for finite and digital signals. For example, using a discrete Fourier transform (DFT) or FFT, the frequency resolution, or bin width, is inversely proportional to the total length of the time record being processed. Specifically,

$$\Delta\nu = \frac{1}{T}\ , \tag{15}$$

where T is the length of the record (in seconds) and $\Delta\nu$ is the frequency bin width (in hertz). For example, if one needed to track a signal by taking the FFT every tenth of a second, frequency bins would be 10 Hz wide with an uncertainty of ± 10 Hz. This makes

it very difficult to see how a transient signal shifts in frequencies over a short period of time. One may misunderstand that this bin width is the fundamental limit to the resolution one may obtain, due to the uncertainty principle, but it is a specific limit imposed by the nature of the algorithm. Other transformations or signal analyses can potentially obtain higher resolution. Some variations of the FFT have been proposed, which attempt to better minimize uncertainty in the case of processing harmonic or musical signals. Pielemeier and Wakefield introduced a modal distribution that has worked quite successfully on musical signals, which improves on the Wigner distribution by minimizing bias introduced by unwanted cross products in the computation, thus enormously increasing the reliability of the method.[13] However, the modal distribution still does not yield enough resolution for our purposes. On the other hand, the instantaneous frequency (IF) method inherently yields near-perfect resolution in time and frequency, yet may be highly susceptible to bias errors from several sources, especially noise. We found that for our experiment these biases could be controlled well enough to achieve good reliability along with the high resolution.

The IF method inherently has high resolution because of its very nature. It is misleading to think of IF as a decomposition of a signal into its various sinusoids, as with the Fourier transform. To understand the difference, we remember that any signal $f(t)$ may be expressed in analytic form as

$$f(t) = A(t)e^{i\phi(t)}, \tag{16}$$

where A and ϕ are both functions of the independent variable (time in this case). The instantaneous frequency of $f(t)$ is defined to be the time derivative of the phase ϕ (divided by 2π, if expressed in Hz instead of radians). Thus, a FFT of a digital signal produces an output corresponding to the entire time of the signal and over a wide range of frequencies, with a resolution limited by the time length of the signal, whereas the IF of a digital signal produces a single output corresponding to each sample of the signal. Therefore, the main disadvantage (for our purposes) of IF is that no matter how complex a signal may be, we can only read one “frequency” that depends on all the frequency content,

since IF gives the time derivative of the overall phase. This means that to successfully implement IF we must carefully employ an appropriate band-pass filter over the partial of interest in order to obtain a nearly sinusoidal signal.

The basic steps of obtaining the IF of a real digital signal, as given by Boashash,[8] are:

1. Compute the Fourier transform of the signal.
2. Set the negative and DC components equal to zero in order to make the signal analytic.
3. Apply an appropriate band-pass filter, as necessary, in order to analyze a band-limited signal.
4. Apply the inverse Fourier transform to the analytic frequency domain signal.
5. Obtain the instantaneous phase from its real and imaginary components.
6. Differentiate the instantaneous phase with respect to time and divide by 2π.

The only ambiguous step here is applying the band-pass filter. Rossi and Girolami analyzed the evolution of the amplitude and frequency of the different partials of decaying piano tones using IF.[11] They proposed a Gaussian filter over the partial of interest, noting that it does produce artifacts in the attack portion of the signal.

Because we are especially interested in the attack portion of the recorded signal, we use a Bessel band-pass filter with the IF method to preserve the waveform of the band-limited signal and increase reliability over the attack phase at the beginning of the signal, since this portion contains the greatest energy correction to the frequency. To determine the Bessel filter's reliability, a finite digital sinusoid was generated with a frequency of 26.234 Hz, for a 10 second duration and sampled at 44.1 kHz. The IF of the same signal, but with the application of rectangular (in the frequency domain), Gaussian, and 5^{th} order Bessel filters, respectively, appear in Figs. 2 through 4. The cutoff frequencies are chosen to include nearly the entire width of the signal in the frequency domain. The rectangular

filter is included to see how susceptible the IF method can be to any distortion of the waveform. It is easily seen from Fig. 2 that the filter choice is critical to the accuracy of the IF. Over most of the time window, both the Gaussian filter and the Bessel filter provide extremely accurate IFs. However, the Bessel filter maintains its accuracy during the entire initial portion, whereas the Gaussian filter introduces a large bias for the first few tenths of a second. The Bessel filter introduces much more bias during the last second than does the Gaussian, but for decaying tones this portion can be ignored.

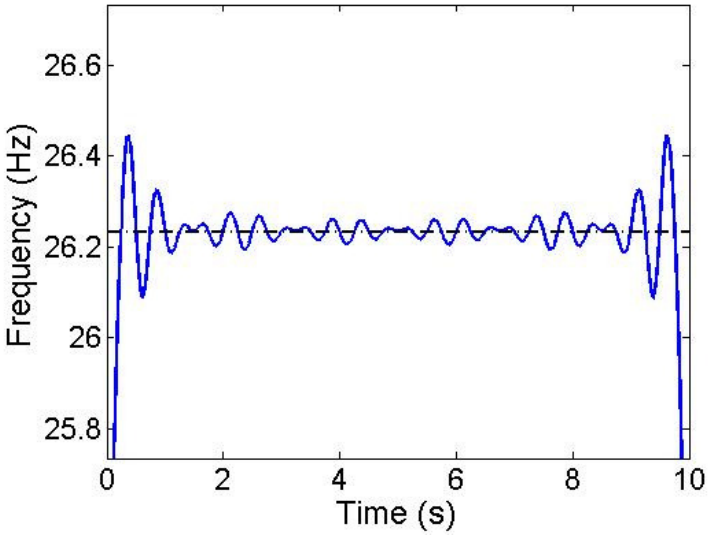

FIG. 2. The instantaneous frequency of a sinusoid (26.234 Hz), using a rectangular filter (in the frequency domain). The dashed line marks 26.234 Hz.

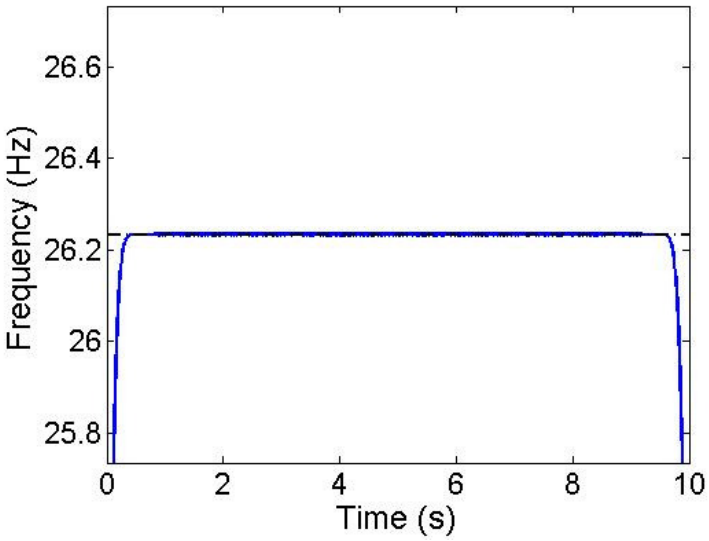

FIG. 3. The instantaneous frequency of a sinusoid (26.234 Hz), using a Gaussian filter. The dashed line marks 26.234 Hz.

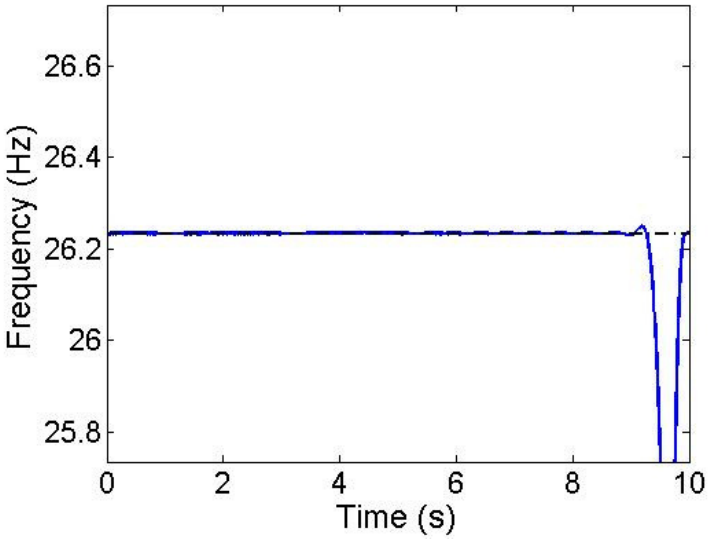

FIG. 4. The instantaneous frequency of a sinusoid (26.234 Hz), using a Bessel filter. The dashed line marks 26.234 Hz.

IV. Experiment

It is not necessary to measure the displacement of a freely vibrating string across its entire length in order to determine its total energy. The following mathematical argument shows that only the velocity and slope of a single point on the string is sufficient (though to obtain the slope, one must observe the neighboring points), as long as the decay is not extremely rapid. Morse and Ingard show that the total energy in the string E, due to its vertical motion, is given by[3]

$$E = \int_0^l \left(\frac{1}{2}\mu \left(\frac{\partial y}{\partial t} \right)^2 + \frac{1}{2} T \left(\frac{\partial y}{\partial x} \right)^2 \right) dx \,. \tag{17}$$

Since we know the solution $y(x,t)$, we can evaluate Eq. (17) as follows:

$$y(x,t) = \sum_{n=1}^{\infty} a_n \sin\left(\frac{n\pi x}{l} \right) \cos\left(\frac{n\pi c t}{l} - \phi_n \right) ,$$

$$\frac{\partial y}{\partial x} = \sum_{n=1}^{\infty} \frac{n\pi a_n}{l} \cos\left(\frac{n\pi x}{l} \right) \cos\left(\frac{n\pi c t}{l} - \phi_n \right) ,$$

$$\left(\frac{\partial y}{\partial x} \right)^2 = \sum_{n=1}^{\infty} \left(\frac{n\pi a_n}{l} \right)^2 \cos^2\left(\frac{n\pi x}{l} \right) \cos^2\left(\frac{n\pi c t}{l} - \phi_n \right) \tag{18}$$

$$+ \sum_{n=1}^{\infty} \sum_{\substack{m=1 \\ m \neq n}}^{\infty} \left(\tfrac{m\pi a_m}{l} \right) \left(\tfrac{n\pi a_n}{l} \right) \cos\left(\tfrac{m\pi x}{l} \right) \cos\left(\tfrac{n\pi x}{l} \right) \cos\left(\tfrac{m\pi c t}{l} - \phi_m \right) \cos\left(\tfrac{n\pi c t}{l} - \phi_n \right) ,$$

$$\frac{\partial y}{\partial t} = -c \sum_{n=1}^{\infty} \frac{n\pi a_n}{l} \sin\left(\frac{n\pi x}{l} \right) \sin\left(\frac{n\pi c t}{l} - \phi_n \right) ,$$

$$\left(\frac{\partial y}{\partial t} \right)^2 = c^2 \sum_{n=1}^{\infty} \left(\frac{n\pi a_n}{l} \right)^2 \sin^2\left(\frac{n\pi x}{l} \right) \sin^2\left(\frac{n\pi c t}{l} - \phi_n \right) \tag{19}$$

$$+ c^2 \sum_{n=1}^{\infty} \sum_{\substack{m=1 \\ m \neq n}}^{\infty} \left(\tfrac{m\pi a_m}{l} \right) \left(\tfrac{n\pi a_n}{l} \right) \sin\left(\tfrac{m\pi x}{l} \right) \sin\left(\tfrac{n\pi x}{l} \right) \sin\left(\tfrac{m\pi c t}{l} - \phi_m \right) \sin\left(\tfrac{n\pi c t}{l} - \phi_n \right) .$$

Before evaluating the integral in Eq. (17) further, we assume that the energy density (given by the integrand) is the same over one period of oscillation as over any other period of oscillation. This assumption is also valid for the case of a slowly decaying signal, such as those measured in the experiment presented in this section, since the energy is approximately constant over the range of a few oscillations. This permits us to take a time average over the integrand. Time averaging over the cross terms in Eqs. (18) and (19) amounts to zero, and over the squared cosines it yields $1/2$. Remembering that $c^2 = T/\mu$, we find that

$$\begin{aligned}\left\langle \left(\frac{\partial y}{\partial x}\right)^2 \right\rangle_t &= \frac{1}{2}\sum_{n=1}^{\infty}\left(\frac{n\pi a_n}{l}\right)^2 \cos^2\left(\frac{n\pi x}{l}\right) , \\ \left\langle \left(\frac{\partial y}{\partial t}\right)^2 \right\rangle_t &= \frac{1}{2}c^2\sum_{n=1}^{\infty}\left(\frac{n\pi a_n}{l}\right)^2 \sin^2\left(\frac{n\pi x}{l}\right)\end{aligned} \tag{20}$$

and

$$\begin{aligned}&\frac{1}{2}\mu\left\langle \left(\frac{\partial y}{\partial t}\right)^2 \right\rangle_t + \frac{1}{2}T\left\langle \left(\frac{\partial y}{\partial x}\right)^2 \right\rangle_t \\ &\quad = T\sum_{n=1}^{\infty}\left(\frac{n\pi a_n}{2l}\right)^2\left(\sin^2\left(\frac{n\pi x}{l}\right)+\cos^2\left(\frac{n\pi x}{l}\right)\right) \\ &\quad = T\sum_{n=1}^{\infty}\left(\frac{n\pi a_n}{2l}\right)^2 ,\end{aligned} \tag{21}$$

which is constant in x, and can be pulled out of the integral in Eq. (17). Evaluating the integral then simply produces an l, and the total energy is the same for any value of x, as long as it is time averaged over one period. Therefore, we are able to calculate the energy, after measuring the slope and displacement of a very small section of the string, according to the formula

$$\frac{E}{T_0 l} \approx \frac{E}{Tl} = \frac{1}{2}\left(\frac{1}{c^2}\left\langle\left(\frac{\partial y}{\partial t}\right)^2\right\rangle + \left\langle\left(\frac{\partial y}{\partial x}\right)^2\right\rangle\right). \tag{22}$$

To measure both the IF and the total energy in a freely vibrating string, Röslau piano wire was strung across a monochord apparatus and high speed video was taken of a small portion of the string during and after the pluck. An acoustic recording of the plucked string sound was made simultaneously during one of the tests. Figure 5 shows a photograph of the experimental setup, and Fig. 6 shows a simple two-dimensional schematic of the experimental setup. The camera recorded 7.2 seconds of data at 9000 frames per second (fps) for each trial, while it was positioned at about 1/10 the speaking length from the left termination point. It had a window of height 12 mm and width 1.5 mm (512 x 64 pixels, grayscale). The position scaling of the video frames was determined by the known diameter of the string (0.94 mm) in the picture. The plucking mechanism consisted of a rod which slid through a tight aperture fastened to the base of the monochord apparatus. The rod (1 cm diameter) was positioned so that the string was initially stretched underneath the edge of the rod, and then it was pulled out quickly to pluck the string. The high speed camera recording was started shortly before the pluck. The string was initially displaced 1 cm (the diameter of the rod) from equilibrium at a point a little beyond 1/6 the speaking length from the termination point on the right.

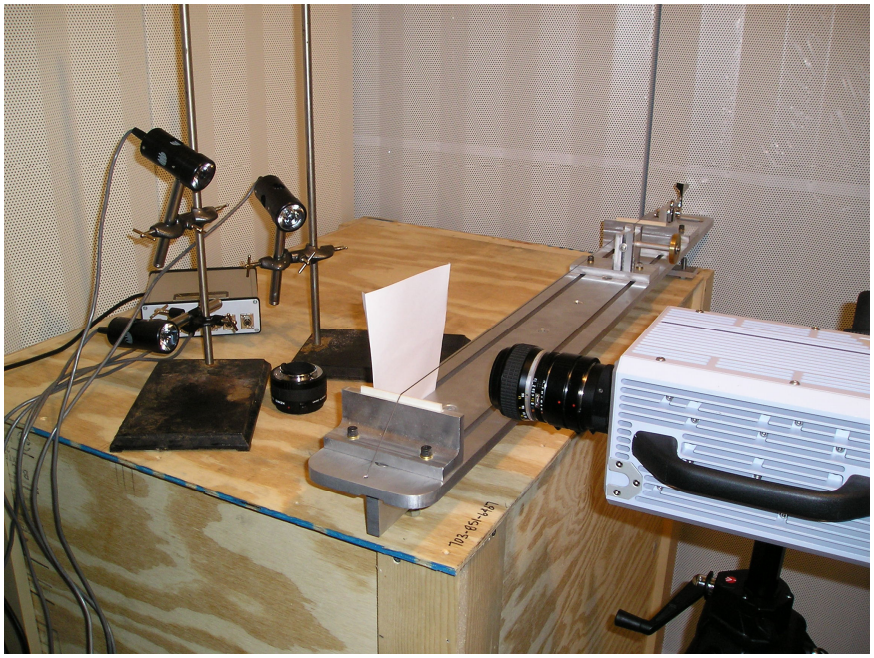

FIG. 5. Experimental setup for a high speed video recording of a plucked piano string on a monochord.

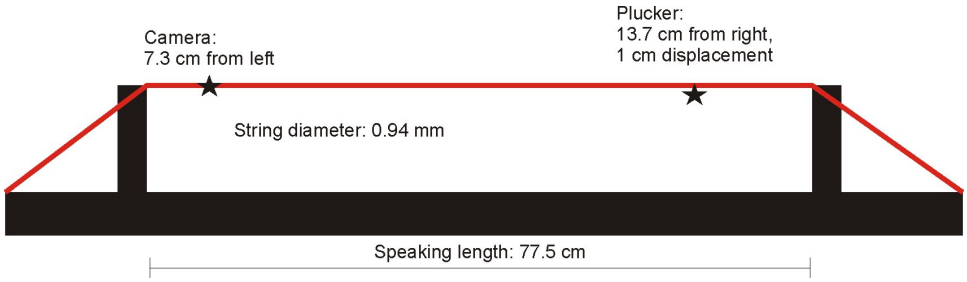

FIG. 6. Schematic of the experimental setup for a high speed video recording of a plucked piano string on a monochord.

The Röslau piano wire was made of steel with a density of 8 g/cm^3 and a Young's modulus of 206 GPa (as reported by the manufacturer). The diameter was measured to be 0.94 mm. The string was stretched to a speaking length of 77.5 cm and an equilibrium tension of approximately 340 N. This last value was calculated using Eq. (5) and measuring the low-amplitude fundamental frequency at 159.6 Hz. The string was plucked hard several times and allowed to settle over a few days in order to stabilize the tension before making any recordings or determining the above-mentioned physical quantities.

Six video recordings were made in total, the first four to capture vertical motion and the last two to capture horizontal motion (by laying the apparatus on its side). Both axes of motion were necessary in calculating the total energy, since some horizontal motion was inevitable. Because we could not simultaneously record both axes of motion, we instead determined how repeatable the pluck was, so that a successive pluck could be treated as if it were the same, once the apparatus was tilted to get horizontal motion. It will be shown later that the repeatability of the pluck was very good for our purposes. During the fourth recording (Test 4), an acoustic recording was also made, using a 1/2-inch condenser ICP microphone positioned within the horizontal plane of the string, at approximately a 45° angle to the length of the string, and 1.5 m from the left termination point. The environment in which the recording was made was hemi-anechoic, but with several other objects in the room that had reflecting surfaces, and with significant background noise, mostly from the backlights for use with the video recordings. The acoustic recording served as a verification that the IFs of the partials were the same, whether it was measured acoustically or directly from the video.

The video was exported as JPEG images and post-processed in MATLAB. The color map was converted from grayscale to jet, for viewing purposes. The slope and position of the string in a given frame was calculated by scanning each column for a cutoff color intensity that best described the top and bottom edges of the string. The positions of these pixels were then fitted to a line, in the least-squares sense, for both the top and bottom edges separately. The displacement of the string was then chosen as the average displacement between the midpoints of the two edges of the string, and the slope was determined as the average of the edges' slopes. Because the camera was not perfectly centered vertically on the string, it was necessary to calibrate both the slope and displacement to equilibrium by using the average values of these over the last 100 oscillations (during low-amplitude vibration where the displacement should average to zero). The displacement velocity was then calculated by using the center difference formula for the derivative of a digitized signal y,

$$\dot{y}_n = \frac{y_{n+1} - y_{n-1}}{2\Delta t}, \tag{23}$$

where n denotes the sample number and Δt is the sampling period.

Figure 7 shows the first several frames after excitation for Test 4. As is evident from the figure, the faster string movement yields blurrier images, so it is necessary to verify the reliability of the calculated edges. A close-up of one of the blurriest frame images is shown in Fig. 8, along with the raw extraction data (blue dots) and the linear fits (black lines) for the string edges. Two questions arise in considering the reliability of the data extraction: (1) how good are the linear fits, and (2) how much do the slopes of the top and bottom edges differ? The linear fits are very good over all frames of the 6 tests, with the average standard deviation of the data from the fits being 0.02230 pixels and the maximum being 0.24085, so that the reliability of the linear fits lies well within the limits of our 1 pixel resolution. On the other hand, the differences in slope between the top and bottom edges are a bit high. We choose 1/64=0.01563 as our resolution limit for the slope (since we can count across 64 pixels and up 1, and still detect a slope). The average difference in slope for all 6 tests is 0.01025, which is within our slope resolution limit, but there are many frames with much greater differences, 0.19020 being the highest. See Fig. 8 for example—not only are the slopes of the edges different, but one edge is distinctly positive while the other edge is distinctly negative. For these blurry images, this discrepancy in the two slopes is most likely due to the fact that, just like the displacement, the slope is also changing significantly over the period it takes to capture the frame. This is why Fig. 8 is blurrier on the left side than on the right, since the right side of the string moved a greater distance than the left side over that amount of time. Therefore, it makes sense that even with somewhat different slopes for the two edges, their average would be representative of the center of the string. Thus, the edge extraction is adequately reliable for calculating the velocity and slope of the string from video.

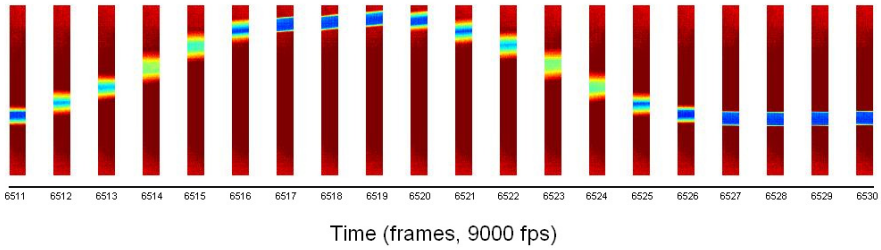

FIG. 7. Frames 6511 to 6530 of Test 4 video at 9000 fps, immediately after excitation of the string.

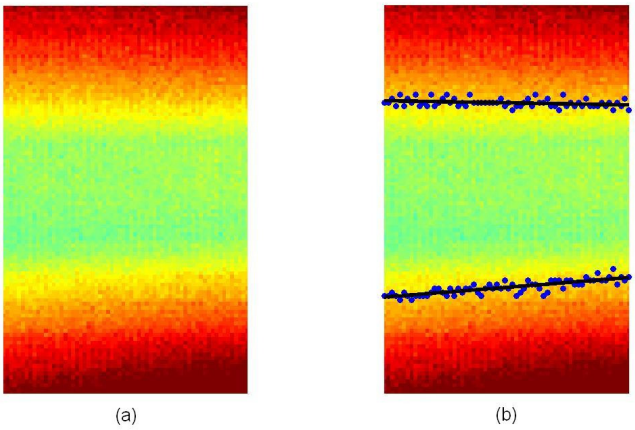

FIG. 8. Close-up of frame 6514 of Test 4 (a) by itself, and (b) with raw data (blue dots) and linear fits (black lines) for the top and bottom edges of the string.

V. Results

Before comparing the experimental measurements of the frequencies to the theoretical predictions, it is first necessary to verify the repeatability of the pluck so that we can add horizontal and vertical energies together, even though they were measured in different recordings. Figures 9 and 10 show the first few oscillations of the vertical and the horizontal displacements versus time for each test, respectively. Figures 11 and 12 then show the same respective plots, but approximately one second later. The plots reveal that the different tests start out almost exactly the same, but are out of phase later on. However, at this later point in time, the vertical tests still hold similar shapes, while the horizontal tests do to some degree. Since we are only concerned with the energy (averaged over each period) being the same for each test for a given direction of motion, phase mismatch should not result in any significant disagreement.

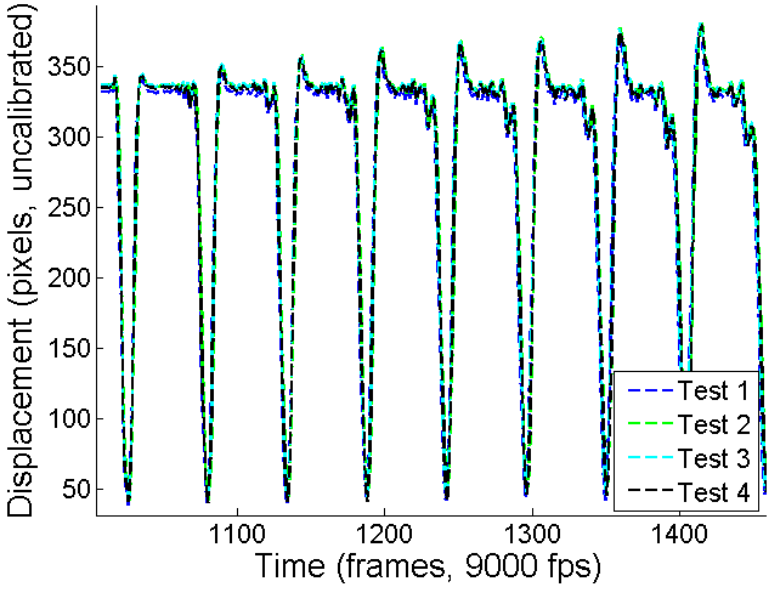

FIG. 9. The first few oscillations of vertical motion of the string for Tests 1-4.

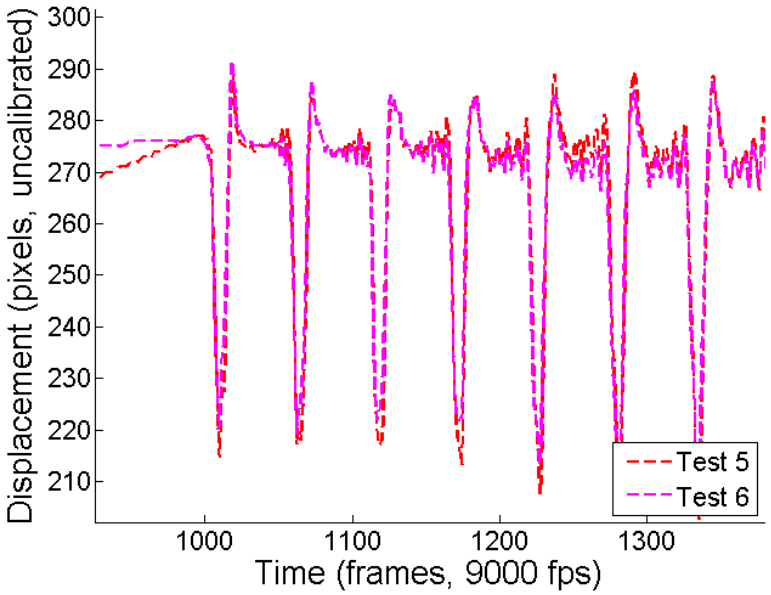

FIG. 10. The first few oscillations of horizontal motion of the string for Tests 5 and 6.

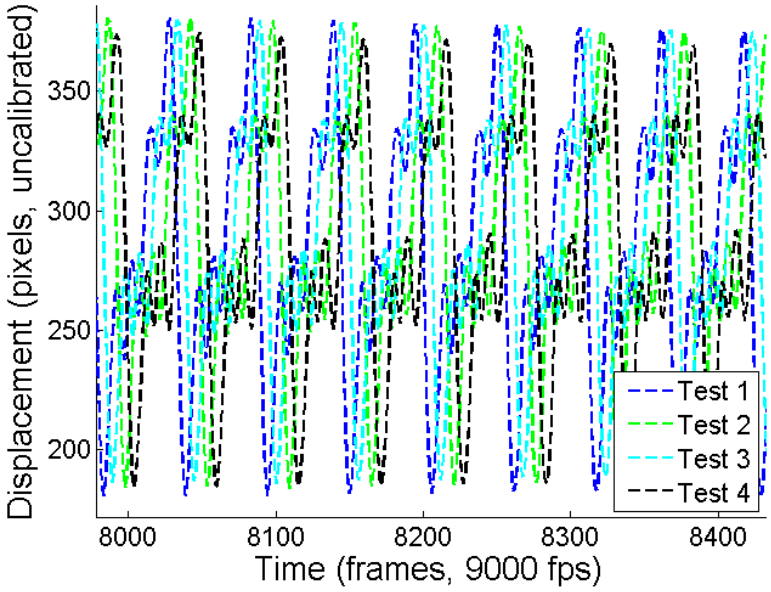

FIG. 11. A few oscillations of vertical motion of the string for Tests 1 through 4 about 1 second after excitation.

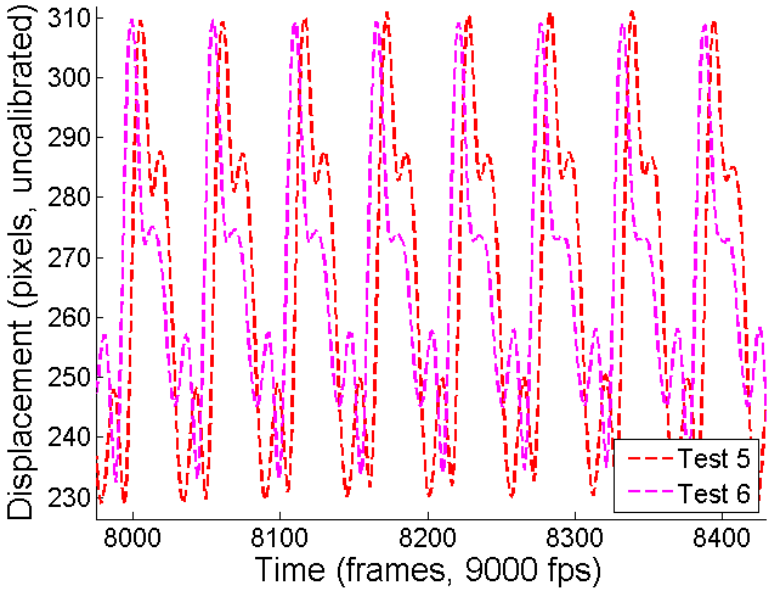

FIG. 12. A few oscillations of horizontal motion of the string for Tests 5 and 6 about 1 second after excitation.

We can evaluate the energy correlation between the different tests directly. The dimensionless parameter $E/T_0 l$ is plotted for the several tests in Figs. 13 and 14, for vertical and horizontal motion, respectively. The energy for Test 1 is slightly greater than that of Tests 2, 3 and 4, but not enough to be a concern. Tests 5 and 6 are also relatively close. To quantify the correlation, we compare standard deviations between the energies of each test with the maximum energy observed, $E_{\max}/T_0 l = 6.1\times10^{-4}$. The maximum difference between any two tests of the same direction of motion is found to be 8.273×10^{-5}, and the maximum standard deviation is $\sigma_{\max} = 1.367\times10^{-5}$. If Test 1 is thrown out, the maximum difference is 6.057×10^{-5} and the maximum standard deviation $\sigma_{\max} = 7.536\times10^{-6}$. Comparing this last number to the maximum energy observed, $\sigma_{\max}/E_{\max} = 0.0124$, which represents very high correlation.

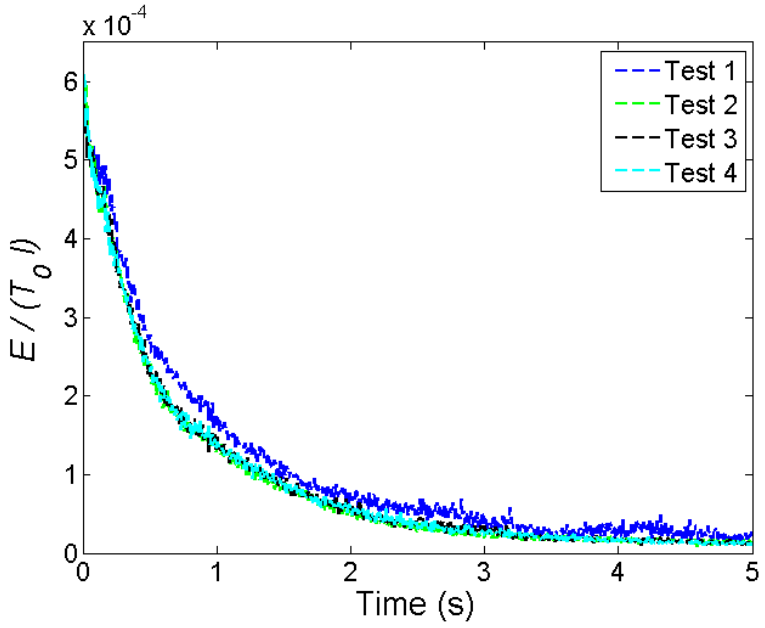

FIG. 13 The energy in the string (divided by $T_0 l$) versus time for Tests 1-4 (vertical motion).

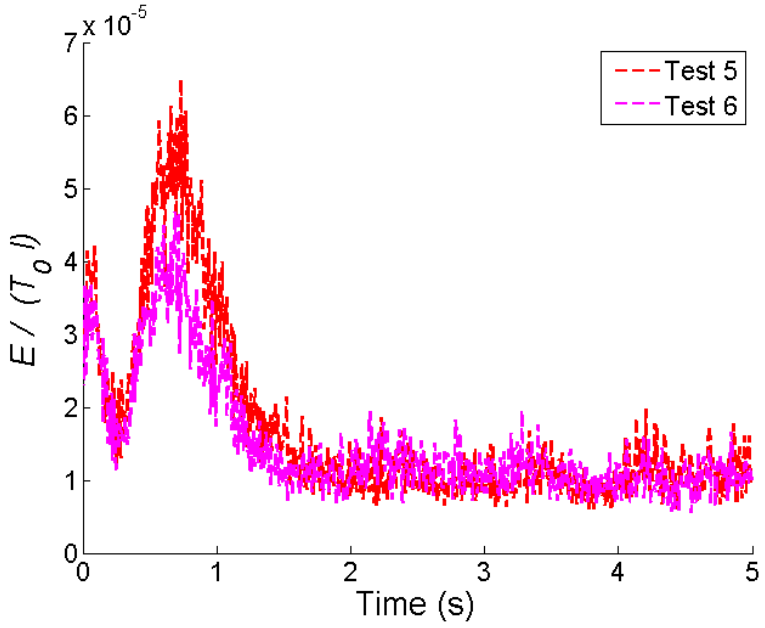

FIG. 14 The energy in the string (divided by $T_0 l$) versus time for Tests 5 and 6 (horizontal motion).

It is reasonable to assume that the IF measured from the acoustic signal is the same as that measured directly from the string displacement taken from the video. The primary differences would arise from noise. To verify this, we compare the audio and video IF for Test 4, partials 1 and 5 in Figs. 15 and 16, respectively. These figures demonstrate that the audio signal is much noisier (fan noise from the back lights, etc.), which severely distorts its IF. The video IF clearly represents the same signal, only with very little noise. Similar results are observed for other partials. Thus, we use the video IF when comparing the measurements to the theoretical model.

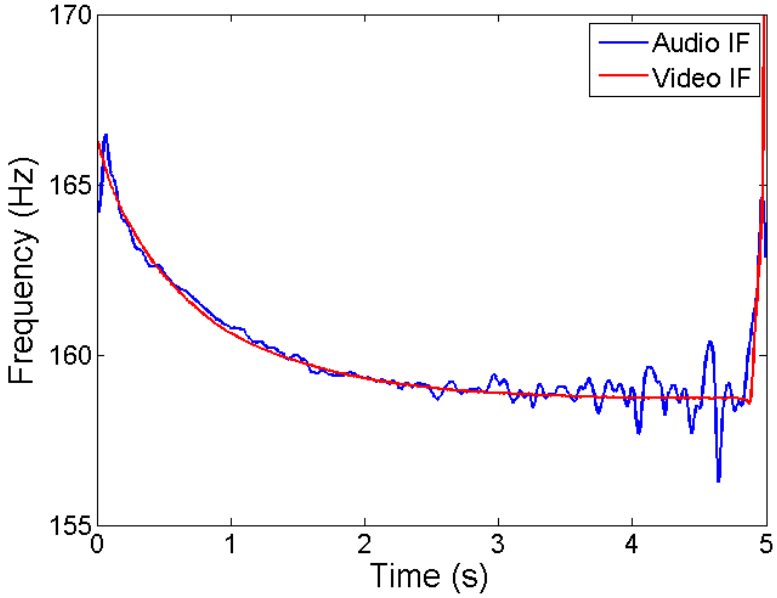

FIG. 15. Comparison of audio and video instantaneous frequencies for the fundamental (1st partial).

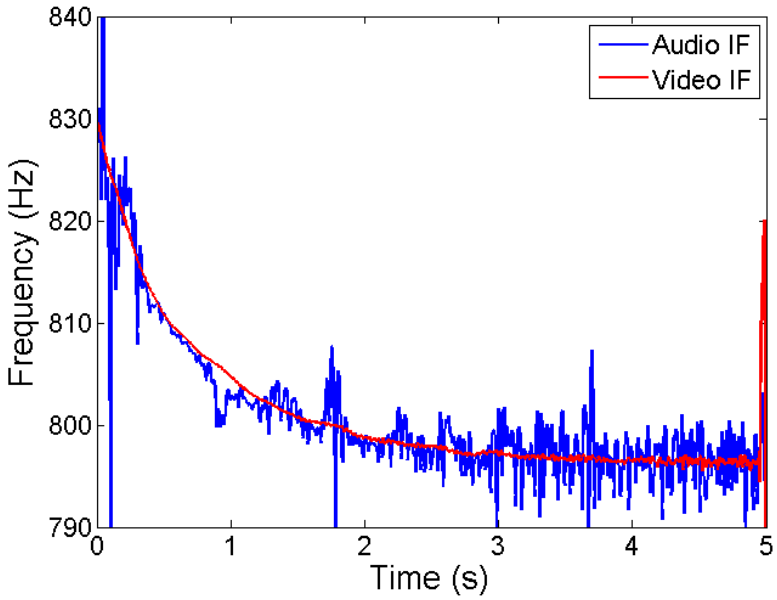

FIG. 16. Comparison of audio and video instantaneous frequencies for the 5th partial.

We now compare the measured IF with the predicted values dependent on the total energy in the string (as explained in Section II). To calculate the total energy, we add the measured energies of Test 4 (vertical motion) and Test 5 (horizontal motion) and average over each 6.26566 ms (approximately one period). To obtain the measured frequency drift, we convert the absolute IFs to cents. This requires an estimate of the stable frequencies; however, there was always some amount of energy in the string throughout the test, as it was not allowed to vibrate indefinitely until it came to rest during the recording. This yields some deviation from the equilibrium frequencies in the theoretical model at low amplitudes. Thus, we choose the stable frequencies corresponding to the IFs of the partials for optimal agreement with the model at the tail end of the recorded signal.

Figure 17 plots partials 1 through 8 in cents next to the theoretical model, using input from the energy measurements. The partials deviate from their stable values very similarly to each other. This would be expected since, according to the theory, the deviation should not have any dependence on the partial number. At later times in the recording, below about 20 cents, the model data agrees very well with the measured partial frequencies, but at higher amplitudes in the attack phase of the signal the model data overshoots by as much as 29% of the measured partial frequencies. In order to better see how much the model data deviates, Fig. 18 shows the difference in cents between the 1st partial and the model's prediction. Here, we can see that even in the range between about 20 and 40 cents (from 0.5 to 1 s on the time axis), the model is still only about 5 cents sharp relative to the measured values. Thus the model predicts the change in frequency fairly accurately except for very large vibration amplitudes.

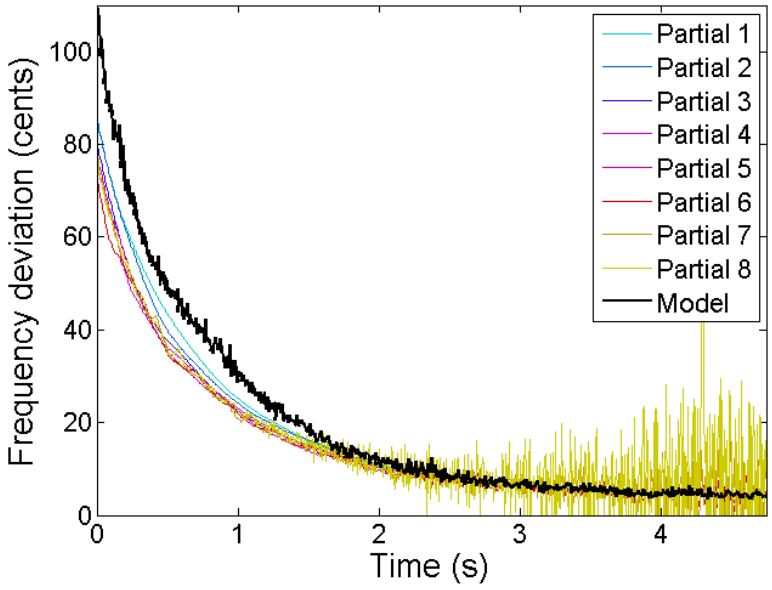

FIG. 17. The instantaneous frequencies (in cents) of partials 1 through 8 of Test 4 plotted against the model prediction based on energies measured from Test 4 (vertical motion) and Test 5 (horizontal motion).

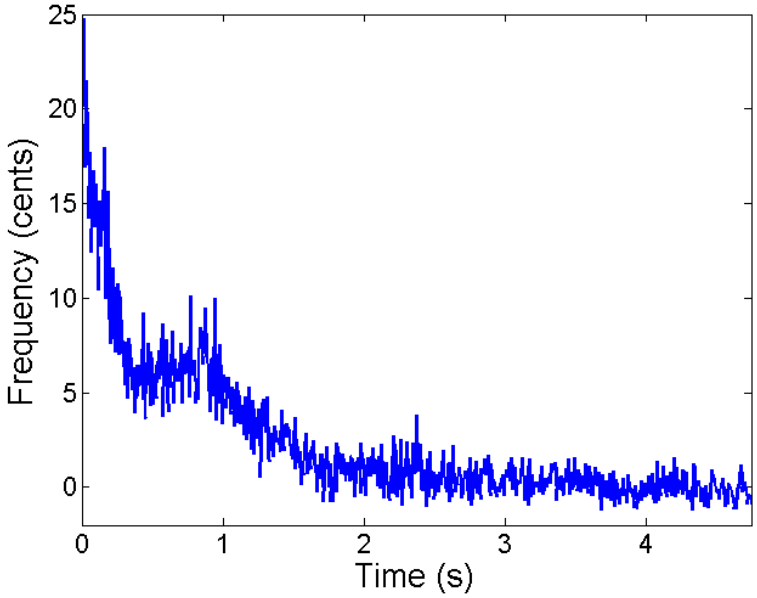

FIG. 18. Difference (in cents) between the instantaneous frequency of the fundamental (1st partial) and the model prediction based on energies measured from Test 4 (vertical motion) and Test 5 (horizontal motion).

VI. Conclusions

The theoretical model proposed in this work introduced a correction to the normal frequencies (partials) of a freely vibrating string, derived from the second-order wave equation, that is proportional to the total energy in the string. The model employed time and spatial averages of the dynamic tension, instead of the commonly used equilibrium tension, and showed that these averages produce a correction term that is proportional to the total energy in the string. To test the model, a high speed video recording was made of a vibrating string, from which the IFs of the partials were extracted (using a band-pass Bessel filter for each partial) and also the total energy of the string, both as functions of time. The Bessel filter was chosen in conjunction with the IF method based on the IF measured for a finite sinusoid of known frequency, using the Bessel filter and others for comparison. As long as the noise level was low (as was the case for the first several partials extracted from the video), the IF method with the Bessel filter proved to be very reliable. The total energy was calculated by extracting the slope and velocity of a small portion of the string, giving the total energy density at that point, which was then averaged over each period of oscillation. This time averaged energy density produced a uniform value over the entire length of the string. This method of measuring the energy made it possible to get high resolution on a very small portion of the string, rather than capturing video of the entire length of the string.

The comparison of results showed that the partial frequencies indeed are much sharper at higher displacement amplitudes, and the theoretical model accurately predicts this correction up to about 40 cents. Beyond this, the model overshoots somewhat significantly. The measured IFs of the partials deviated as much as 83 cents at the beginning of the pluck, almost an entire semitone, where the string was initially displaced by only about 1 cm at the position of the plucker. Smaller initial displacements can cause a

string's partial frequencies to deviate by a few cents, which is detectable by the human ear and can significantly affect the tuning of musical instruments.

More rigorous methods for extracting the energy in the string may be necessary in order to more accurately form the theoretical model. Further research into the problem of a string vibrating at large amplitudes may look into the effect the dynamic tension has on the differential equation when it is not approximated as a constant. Also, including Fletcher's fourth-order term in the differential equation may produce a more accurate model. These investigations could lead to higher-order corrections to the frequencies that are valid at very large amplitudes. Finally, further research into the effect of mode coupling and multiple-string coupling on normal frequencies may prove to be useful in application to real musical instruments.

References

[1] H. Fletcher, "Normal vibration frequencies of a stiff piano string," J. Acoust. Soc. Am. **36(1),** 203-209 (1964).

[2] B. E. Anderson and W. J. Strong, "The effect on pitch due to the inharmonicity of piano tones," J. Acoust. Soc. Am. **117(5)**, 3268-3272 (2005).

[3] P.M. Morse and K.U. Ingard, *Theoretical Acoustics,* (New York, McGraw Hill, 1968).

[4] G.V. Anand, "Large-amplitude damped free vibration of a stretched string," J. Acoust. Soc. Am. **45(5),** 1089-1096 (1969).

[5] S. Bilbao, "Conservative numerical methods for nonlinear strings," J. Acoust. Soc. Am. **118(5),** 3316-3327 (2005).

[6] J. Carson and T. Fry, "Variable frequency electric circuit theory with application to the theory of frequency modulation," *Bell System Tech. J.*, vol. 16, pp. 513-540, 1937.

[7] J. Ville, "Theorie et application de la notion de signal analytic," *Cables et Transmissions*, vol. 2A(1), pp. 61-74, Paris, France, 1948. Translation by I. Selin, "Theory and applications of the notion of complex signal," Report T-92, RAND Corporation, Santa Monica, CA.

[8] B. Boashash, "Estimating and interpreting the instantaneous frequency of a signal—Part 1: Fundamentals," Proc. IEEE **80(4),** 520-538 (1992).

[9] B. Boashash, "Estimating and interpreting the instantaneous frequency of a signal—Part 2: Algorithms and Applications," Proc. IEEE **80(4),** 540-568 (1992).

[10] H. Suzuki, F. Ma, H. Izumi, O. Yamazaki, S. Okawa and K. Kido, "Instantaneous frequencies of signals obtained by the analytic signal method," Acoust. Sci. & Tech. **27(3),** 163-170 (2006).

[11] L. Rossi and G. Girolami, "Instantaneous frequency and short term Fourier transforms: Application to piano sounds," J. Acoust. Soc. Am. **110(5),** 2412-2420 (2001).

[12] A.P. French, *Vibrations and Waves,* (New York, W.W. Norton & Company, 1971).

[13] W.J. Pielemeier and G.H. Wakefield, "A high-resolution time-frequency representation for musical instrument signals," J. Acoust. Soc. Am. **99(4),** 2382-2396 (1996).

Appendix A: Derivation of dynamic tension

Consider a small portion of a free vibrating string similar to that shown in Fig. 1. Hooke's law states that the tension is

$$T = \frac{QA}{dl_0}\Delta l\,, \tag{A.1}$$

where Q is Young's modulus, A is the cross-sectional area of the wire, dl_0 is the natural string length under zero tension and Δl is the change in length under tension T, assuming any change in A is negligible. Let the piece of string have length dx under equilibrium tension T_0. Then

$$T_0 = QA\frac{dx - dl_0}{dl_0} = QA\left(\frac{dx}{dl_0} - 1\right), \tag{A.2}$$

from which we find that

$$\frac{dx}{dl_0} = \frac{T_0}{QA} + 1\,. \tag{A.3}$$

When in motion, the two ends of the piece of string are now located at $\mathbf{p}_1 = (x + \xi, \eta, \zeta)$ and $\mathbf{p}_2 = (x + dx + \xi + d\xi, \eta + d\eta, \zeta + d\zeta)$, and its length is given by

$$\begin{aligned} dl = |\mathbf{p}_2 - \mathbf{p}_1| &= \sqrt{(dx + d\xi)^2 + (d\eta)^2 + (d\zeta)^2} \\ &= \sqrt{\left(1 + \frac{\partial\xi}{\partial x}\right)^2 + \left(\frac{\partial\eta}{\partial x}\right)^2 + \left(\frac{\partial\zeta}{\partial x}\right)^2}\,dx\,, \end{aligned} \tag{A.4}$$

where $\mathbf{r}(x,t) = \xi\mathbf{e}_x + \eta\mathbf{e}_y + \zeta\mathbf{e}_z$ is the three-dimensional displacement vector from equilibrium. The length dl can also be expressed in terms of the position vector

$$\mathbf{R}(x,t) = x\mathbf{e}_x + \mathbf{r}(x,t),$$

$$dl = \left|\frac{\partial \mathbf{R}}{\partial x}\right| dx, \tag{A.5}$$

Substituting Eq. (A.5) into Eq. (A.1), and making use of Eq. (A.3), the dynamic tension is

$$\begin{aligned} T(x,t) &= QA\left(\left|\frac{\partial \mathbf{R}}{\partial x}\right|\frac{dx}{dl_0} - 1\right) \\ &= QA\left(\left|\frac{\partial \mathbf{R}}{\partial x}\right|\left(\frac{T_0}{QA} + 1\right) - 1\right) \\ &= \left|\frac{\partial \mathbf{R}}{\partial x}\right|(T_0 + QA) - QA \\ &= T_0 + (T_0 + QA)\left(\left|\frac{\partial \mathbf{R}}{\partial x}\right| - 1\right). \end{aligned} \tag{A.6}$$

In practice, $T_0 << QA$, and Morse and Ingard's formula[3] is confirmed:

$$T(x,t) = T_0 + QA\left(\left|\frac{\partial \mathbf{R}}{\partial x}\right| - 1\right). \tag{A.7}$$

Appendix B: Introducing energy into the tension formula

Eq. (10) claims that

$$\left\langle \left\langle \left(\frac{\partial y}{\partial x} \right)^2 \right\rangle_t \right\rangle_x = \frac{E}{Tl}, \tag{B.1}$$

for a given transverse dimension y, where E is the energy (kinetic plus potential) in the string due to that dimension, T is the tension, l is the string length and the angular brackets denote time and spatial averages. This result is obtained by simply performing operations on the solution to the wave equation:

$$\begin{aligned} y(x,t) &= \sum_{n=1}^{\infty} a_n \sin\left(\frac{n\pi x}{l}\right)\cos\left(\frac{n\pi ct}{l} - \phi_n\right) \\ \frac{\partial y}{\partial x} &= \sum_{n=1}^{\infty} \frac{n\pi a_n}{l}\cos\left(\frac{n\pi x}{l}\right)\cos\left(\frac{n\pi ct}{l} - \phi_n\right) \\ \left(\frac{\partial y}{\partial x}\right)^2 &= \sum_{n=1}^{\infty}\left(\frac{n\pi a_n}{l}\right)^2 \cos^2\left(\frac{n\pi x}{l}\right)\cos^2\left(\frac{n\pi ct}{l} - \phi_n\right) \\ &\quad + \sum_{n=1}^{\infty}\sum_{\substack{m=1 \\ m\neq n}}^{\infty}\left(\tfrac{m\pi a_m}{l}\right)\left(\tfrac{n\pi a_n}{l}\right)\cos\left(\tfrac{m\pi x}{l}\right)\cos\left(\tfrac{n\pi x}{l}\right)\cos\left(\tfrac{m\pi ct}{l} - \phi_m\right)\cos\left(\tfrac{n\pi ct}{l} - \phi_n\right) \end{aligned} \tag{B.2}$$

In Eq. (B.2), the first sum consists of the squared terms and the double sum consists of the cross terms. Taking the average with respect to time and space amounts to zero for the cross terms (since they are products of orthogonal functions) and each cosine squared in the first sum produces a $1/2$; therefore,

$$\left\langle \left\langle \left(\frac{\partial y}{\partial x} \right)^2 \right\rangle_t \right\rangle_x = \sum_{n=1}^{\infty} \left(\frac{n\pi a_n}{2l} \right)^2 . \tag{B.3}$$

On the other hand, the total energy is found by integrating over the kinetic and potential energy densities:

$$E = \int_0^l \left(\frac{1}{2}\mu \left(\frac{\partial y}{\partial t} \right)^2 + \frac{1}{2} T \left(\frac{\partial y}{\partial x} \right)^2 \right) dx .$$

This works out to be[3]

$$E = Tl \sum_{n=1}^{\infty} \left(\frac{n\pi a_n}{2l} \right)^2 . \tag{B.4}$$

Combining Eqs. (B.3) and (B.4),

$$\left\langle \left\langle \left(\frac{\partial y}{\partial x} \right)^2 \right\rangle \right\rangle = \frac{E}{Tl} . \tag{B.5}$$